Korean J. Chem. Eng., 34(7), 2002-2010 (2017)
DOI: 10.1007/s11814-017-0079-0

pISSN: 0256-1115
eISSN: 1975-7220

Influence of feeding mode on cooling crystallization of L-lysine in Couette-Taylor crystallizer

Anh-Tuan Nguyen and Woo-Sik Kim†

Department of Chemical Engineering, ILRI, Kyung Hee University, Seocheon-dong, Giheung-gu, Yongin-si 17104, Korea
(*Received 25 November 2016 • accepted 16 March 2017*)

Abstract−A continuous Couette-Taylor (CT) crystallizer was used to apply a multiple feeding mode strategy to enhance the crystal size and size distribution of L-lysine crystals in cooling crystallization. With a 5-min mean residence time, feed concentration of 900 g/*l*, and rotation speed of 700 rpm, the multiple feeding mode strategy Run-III (D21) produced a large crystal size of 139 μm and coefficient of variation (CV) for the size distribution of 0.39, both of which were significantly enhanced when compared with the conventional feeding mode Run-I (D1) that produced a crystal size of 82 μm and CV for the size distribution of 0.53. Essentially, the crystal size was enhanced around 70%, while the size distribution was improved around 28%. Finally, the impact of the multiple feeding mode strategy on the crystal size and size distribution is explained in terms of effective control of the supersaturation.

Keywords: Multiple Feeding Mode, Taylor Vortex Flow, Couette-taylor Crystallizer, Cooling Crystallization, Nucleation, Growth, Mass Transfer, Heat Transfer

INTRODUCTION

The crystal size and size distribution are important product properties in various fields, such as food additives, pharmaceuticals, and fine chemical materials, as they directly determine the quality, features, and downstream processing efficiency [1]. For example, a large crystal size is advantageous for downstream filtration, washing, centrifuging, and packaging. Meanwhile, a broad size distribution provides different dissolution times for each crystal product. In general, the preferences for crystal products are a large crystal size and narrow size distribution.

Many studies have already attempted to produce solid products with a large crystal size and narrow size distribution. Plus, it is well known that the crystal size and size distribution directly depend on the nucleation and growth process, where a large crystal size with a narrow size distribution can be achieved when crystal growth is promoted and secondary nucleation is suppressed. According to Takahashi et al. [2], the crystal size and size distribution can be controlled by the mixing conditions in the crystallizer using different types of impeller. As such, large crystals with a narrow size distribution can be obtained when using an impeller that produces an axial flow, whereas a bimodal crystal size distribution can be achieved when the impeller produces a radial flow. In the latter case, secondary nucleation and agglomeration are not well suppressed, resulting in a small crystal size and bimodal size distribution. In addition, Liotta et al. [3] reported a large crystal size and narrow size distribution for API when using feed-back control of supersaturation combined with seed crystals in the metastable zone. In this case, the crystal growth process is promoted with negligible secondary nucleation, resulting in a large crystal size and narrow size distribution. Kubota et al. [4] also noted a significantly enhanced crystal size and size distribution when adding a critical amount of seed crystals, regardless of the cooling program. A high amount of seed crystals provides a high surface area that promotes the crystal growth process and rapidly decreases the supersaturation with negligible secondary nucleation, resulting in a large crystal size and narrow size distribution.

The use of a temperature strategy for the dissolution and growth of crystals is currently widely applied to achieve a large crystal size and narrow size distribution. Here, fine crystals are dissolved at a high temperature to support supersaturation for the growth of the surviving large crystals. Plus, when the process is repeated, the crystal size and size distribution are significantly enhanced. For example, Davey et al. [5] reported that an outside-circulation heating strategy is useful for enhancing the crystal size and size distribution in cooling crystallization. Ooshima et al. [6] demonstrated in WWDJ (wet-wall double-jacket) crystallizer that the crystal size and size distribution of L-Aspartic acid crystal products were markedly promoted when using different temperatures with an upper and lower jacket strategy in the crystallizer, where the fine crystals are dissolved using a high temperature for the upper jacket, while supersaturation for the growth of the surviving large crystals is provided using a low temperature for the lower jacket. Finally, Takiyama et al. [7] reported that the crystal size and size distribution can be enhanced when using a repeatable heating and cooling strategy program in cooling crystallization. Kim and Yang suggested two-step crystallization technique for the crystal size control [8].

The unique Taylor vortex flow in a Couette-Taylor (CT) crystallizer has already been demonstrated as a more valuable fluid hydrodynamic for solving various crystallization phenomena when com-

†To whom correspondence should be addressed.
E-mail: wskim@khu.ac.kr
‡This article is dedicated to Prof. Choon Han on the occasion of his retirement from Kwangwoon University.

pared with the random fluid motion in a conventional mixing tank (MT) crystallizer. For example, Kim et al. [9,10] reported that the phase transformation of guanosine 5-monophosphate (GMP) and sulfamerazine (SMZ) was significantly promoted under a Taylor vortex flow in drowning-out and cooling crystallization, respectively, where it was more than four- to eight-times higher than that in a conventional MT crystallizer. In the case of precipitation, the productivity with a small spherical agglomerated battery material is significantly facilitated in a CT crystallizer when compared with that in a MT crystallizer [11]. Also, the problem of flocculation of hairy calcium lactate crystals in drowning-out crystallization with an MT crystallizer is completely solved with a CT crystallizer [12]. In a previous study of the cooling crystallization of L-Lysine, the crystal properties were also significantly enhanced under a Taylor vortex flow in the CT crystallizer when compared with that in the MT crystallizer [13].

In contrast to previous studies, we used a multiple feeding mode strategy to enhance the crystal size and size distribution of L-lysine crystal products in cooling crystallization. Here, the crystal size and CV of the crystal size distribution were 82 μm and 0.53, respectively, according to the conventional feeding mode strategy from a previous study. Plus, since supersaturation is a critical factor to control the crystal size and size distribution, the effect of other operation conditions, such as the coolant direction, cooling temperature, mean residence time, rotation speed, and feed concentration, was also investigated.

EXPERIMENTAL

The L-Lysine material anhydrous monohydrochloride crystal (99% purity) was supplied by CJ Co. (Korea) without any further purification. The L-lysine feed solution was prepared by dissolving the raw material into distilled water, and the feed concentration was varied from 850 to 1,000 g/*l*. The temperature of the feed solution was always fixed at 50 °C.

The Couette-Taylor (CT) crystallizer was composed of two annular cylinders made of stainless steel, where the inner cylinder was rotated by a motor and the outer cylinder was fixed. The radius of the outer cylinder (r_o) was 28 mm, and the geometric crystallizer (d/r_o) and (L/d) were 0.143 and 75, respectively. Here, d was the gap between the outer and inner cylinders, and L was the axial length of the crystallizer. Based on the dimensions of the crystallizer, the

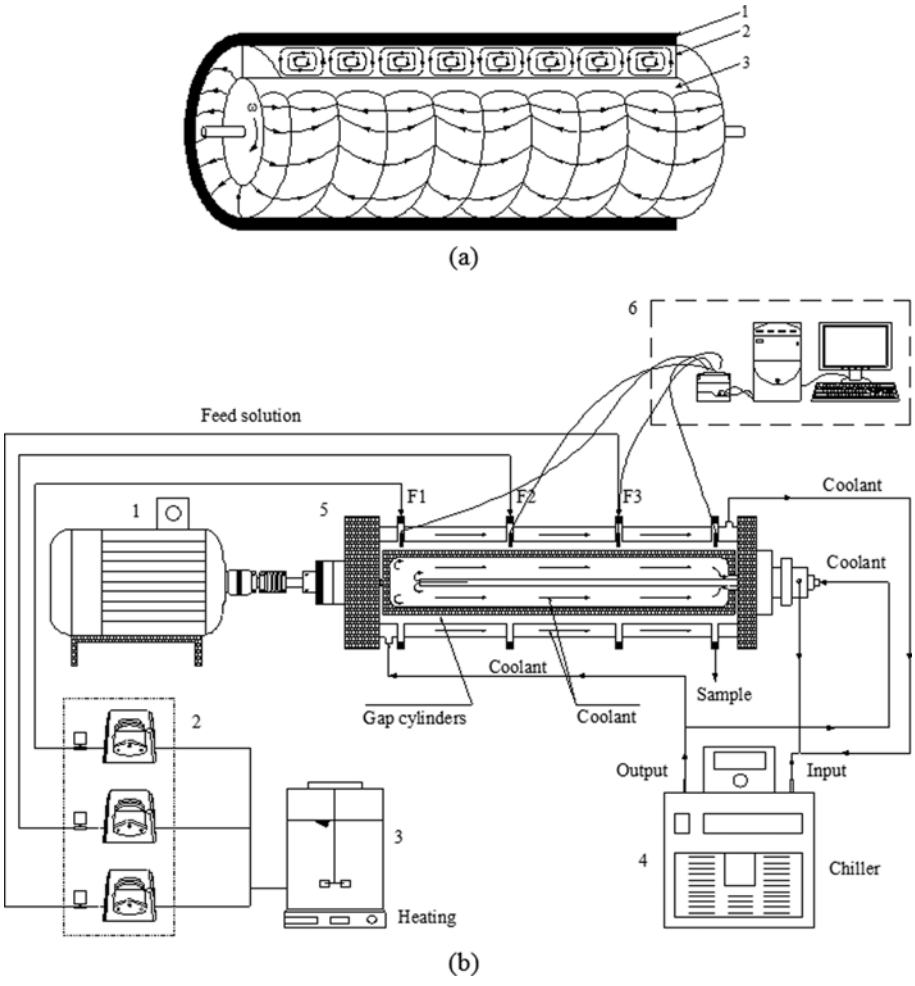

Fig. 1. (a) Schematic drawings of Taylor vortices (1. Stationary outer cylinder; 2. Taylor vortices; 3. Rotating inner cylinder) and (b) experimental system of feeding mode for Couette-Taylor crystallizer (1. DC motor; 2. Pump; 3. L-Lysine feed solution; 4. Chiller; 5. Couette-Taylor crystallizer; 6. Temperature analysis).

working volume was defined as 196 ml. The crystallization of L-lysine was under a Taylor vortex flow induced in the cylinder gap by rotating the inner cylinder. The intensity of the Taylor vortex flow was adjusted by controlling the rotation speed of the motor from 300 to 900 rpm. The Taylor vortex flow and experimental schematics of the conventional and multiple feeding mode strategies are shown in Fig. 1.

The crystallizers were initially filled with the L-lysine feed solution, and the batch mode system was then operated until the suspension temperature approached the cooling temperature. Here, the cooling temperature of the chiller was varied from 15 to 20 °C. During the batch mode cooling crystallization, seed crystals of L-lysine were generated. Thereafter, the continuous operation of L-lysine cooling crystallization was initiated, where the feed solution was directly injected into the crystallizers through inlet ports using pumps (LongerPump, USA). The mean residence time was varied from 2.5 to 20 min by controlling the flow rate of the feed solution from 78.4 to 9.8 ml/min.

Suspension product samples were taken from the crystallizers at the steady state and quickly filtered using a vacuum. The filtered crystals were then dried in a dessicator and analyzed for the crystal size and size distribution (CSD) using a video microscope (IT System, Sometech, USA). To estimate the recovery, the solute concentration and solution temperature were monitored by using a UV-Vis (JASCO, V-570, USA) and Labview (National Instruments, USA), respectively.

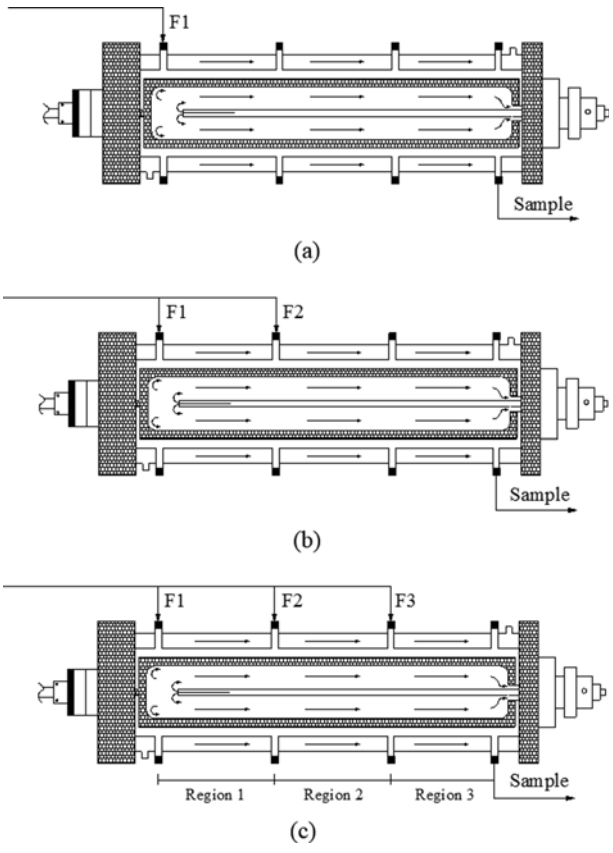

Fig. 2. Schematic of feeding modes in Couette-Taylor crystallizer: (a) Run-I, (b) Run-II, and (c) Run-III.

RESULTS AND DISCUSSION

1. Effect of Multiple Feeding Mode Strategy

To investigate the influence of the multiple feeding mode strategy on the cooling crystallization of L-Lysine, various feeding strategies were applied, as shown in Fig. 2. The conventional feeding mode strategy (Run-I) involved pumping the L-lysine feed solution through inlet ports located at the beginning of the crystallizer, and the product suspension was then obtained at the end of the CT crystallizer (Fig. 2(a)). This feeding mode strategy has already been applied to continuous CT crystallizers in previous studies [12]. In the case of the multiple feeding mode strategy, Run-II and Run-III (Fig. 2(b) and (c)), the L-lysine feed solution was injected through various ports positioned along the axial position of the crystallizer. The total flow rate of the L-lysine feed solution remained fixed for all the feeding mode strategies (Run-I, Run-II, and Run-III).

Crystal size and size distribution depend directly on the nucle-

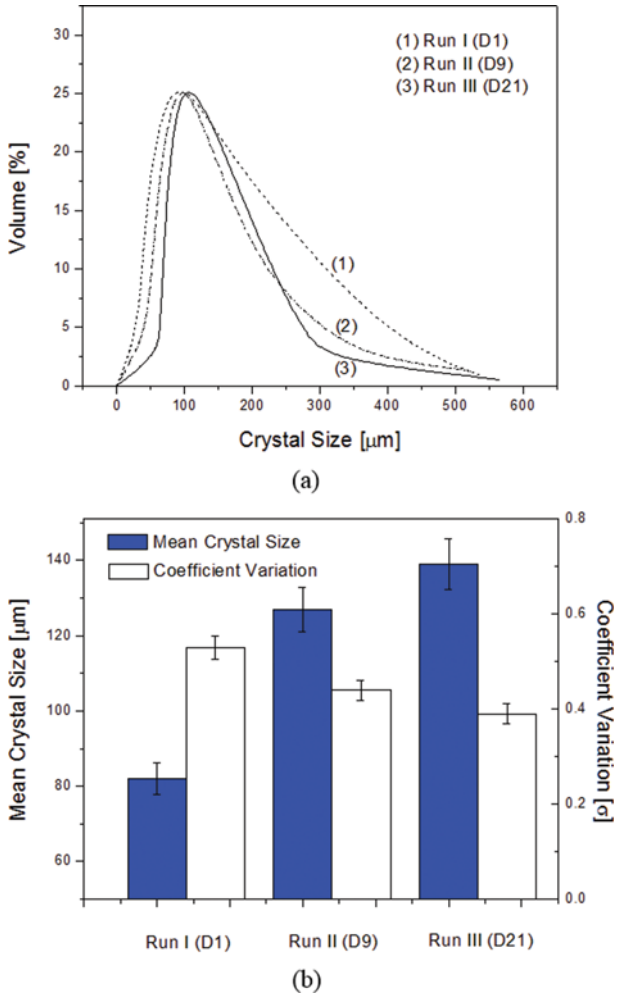

Fig. 3. Typical properties of L-Lysine crystals in cooling crystallization of CT crystallizer with 50 °C feed solution temperature, 20 °C cooling temperature, 700 rpm rotation speed for inner cylinder, 900 g/*l* L-Lysine feed concentration, and 5-min mean residence time. (a) Crystal size distribution, (b) mean crystal size and COV, and (c) recovery.

ation and growth process, both of which are affected by the operation conditions, including the coolant direction, mean residence time, agitation speed, and feed concentration. According to previous studies using the conventional feeding mode strategy (Run-I), the mean crystal size and CV of the crystal size distribution were reported as 82 μm and 0.53, respectively. In the present study, when increasing the mean residence time, the crystal size and CV were both markedly enhanced, yet the productivity of solid products was clearly decreased. Furthermore, when varying the rotation speed or feed concentration, it remained difficult to achieve a large mean crystal and narrow crystal size distribution (small CV). However, the mean crystal size and CV of the L-lysine crystals in the CT crystallizer were significantly enhanced when using the multiple feeding mode strategy. For example, as shown in Fig. 3, when using the distributed feeding mode strategy (Run-II (D9)), the mean crystal size and CV were markedly improved to 127 μm and 0.44, respectively, while the multiple feeding mode (Run-III (D21)) provided a large mean crystal size and small CV of 139 μm and 0.38, respectively, under the same operating conditions. The characteristics of the L-lysine crystals with the different feeding mode strategies are summarized in Table 1.

The effectiveness of the multiple feeding strategy can be explained in terms of the supersaturation in each region of the CT crystallizer. In general, a high-temperature (50 °C) feed solution is rapidly crystallized when injected into a low-temperature (20 °C) crystallizer. Thus, the nucleation rate is obviously determined by the flow rate of the feed solution. However, in the present study, while the total flow rate of the feed (F_T) was the same for all the feeding mode strategies, the regional flow rate (F_i) of the feed distributed along the axial crystallizer varied with the multiple feeding mode strategy. Therefore, when using the conventional feeding mode strategy (Run-I (D1)), the flow rate of the feed solution injected into the first region of the crystallizer was $F_1=F_T$ (ml/min). However, when using the multiple feeding mode strategy Run-III (D21), the regional flow rate of the feed in the crystallizer varied at F_1=70% of F_T in region 1, F_2=20% of F_T in region 2, and F_3=10% of F_T in region 3. The nucleation rate in the first region of the crystallizer was lower with the multiple feeding mode strategy Run-III (D21) than with the conventional feeding mode Run-I (D1). Yet, the seed crystals in the first region grew in the following regions 2 and 3 due to the axial supersaturation continuously created along the crystallizer by the multiple feeding at F_2 and F_3. Here, when the amount of seed crystals in the first region achieved a critical point and the axial supersaturation level was low enough to neglect primary or secondary nucleation during the growth process, the mean crystal size and CV of the L-lysine were enhanced. Otherwise, the mean crystal size and CV were smaller and larger, respectively. For example, when applying the multiple feeding mode Run-II (D3), the mean crystal size and CV were smaller and larger, respectively, than when applying the conventional feeding mode Run-I (D1). This indicates that the high feeding flow rate (F_2=80% of F_T) in region 2 provided a high supersaturation level, initiating significant spontaneous nucleation, plus secondary nucleation was not neglected, resulting in a small mean crystal size and large CV. In present study,

Table 1. Influence of feeding mode on mean crystal size and COV of L-Lysine crystals

Experiments	Distributed feeding symbols	Distributed ratio F1 : F2 : F3	Properties of L-Lysine crystals		Recovery [%]
			Mean crystal size [mm]	Coefficient of variation [s]	
Run-I	D1	1.0 : 0.0 : 0.0	82	0.53	95
Run-II	D2	0.1 : 0.9 : 0.0	68	0.61	95
	D3	0.2 : 0.8 : 0.0	73	0.57	95
	D4	0.3 : 0.7 : 0.0	78	0.55	95
	D5	0.4 : 0.6 : 0.0	85	0.52	95
	D6	0.5 : 0.5 : 0.0	94	0.51	95
	D7	0.6 : 0.4 : 0.0	97	0.50	95
	D8	0.7 : 0.3 : 0.0	104	0.48	95
	D9	0.8 : 0.2 : 0.0	127	0.44	95
	D10	0.9 : 0.1 : 0.0	98	0.49	95
Run-III	D11	0.10 : 0.10 : 0.80	65	0.63	95
	D12	0.10 : 0.20 : 0.70	71	0.60	95
	D13	0.20 : 0.20 : 0.60	80	0.56	95
	D14	0.28 : 0.22 : 0.50	91	0.52	95
	D15	0.30 : 0.30 : 0.40	98	0.50	95
	D16	0.30 : 0.33 : 0.33	105	0.48	95
	D17	0.33 : 0.50 : 0.20	113	0.47	95
	D18	0.40 : 0.40 : 0.20	119	0.47	95
	D19	0.50 : 0.33 : 0.17	121	0.46	95
	D20	0.60 : 0.20 : 0.20	124	0.46	95
	D21	0.70 : 0.20 : 0.10	139	0.38	95
	D22	0.80 : 0.10 : 0.10	110	0.49	95

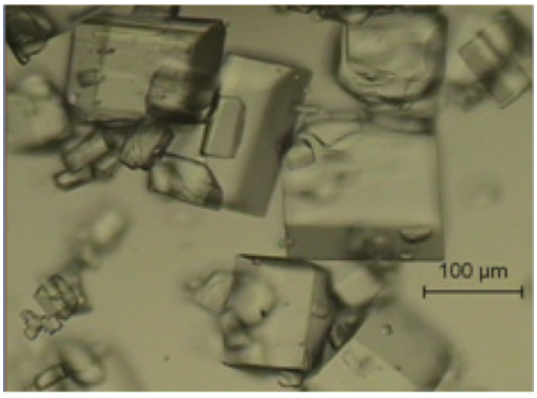

(a)

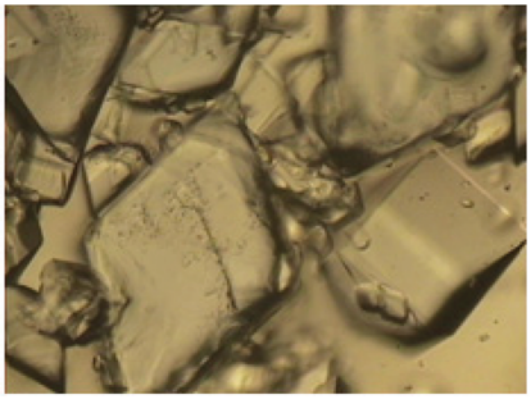

(b)

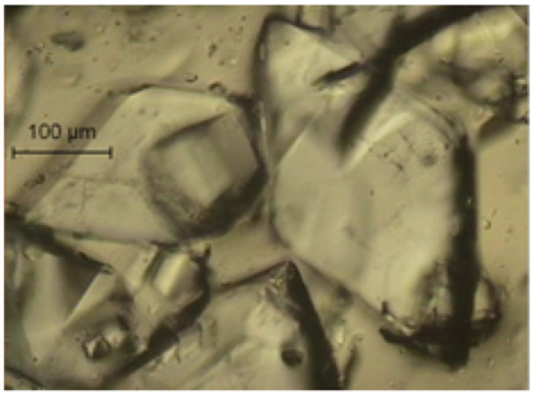

(c)

Fig. 4. Typical morphology of L-Lysine crystals when varying feeding mode in cooling crystallization of CT crystallizer with 50 °C feed solution temperature, 20 °C cooling temperature, 700 rpm rotation speed for inner cylinder, 900 g/*l* L-Lysine feed concentration, and 5-min mean residence time. (a) Run I (D1), (b) Run II (D9), and (c) Run III (D21).

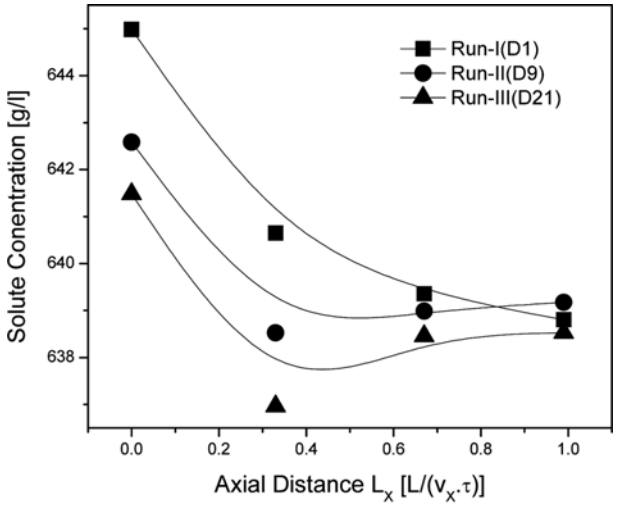

(a)

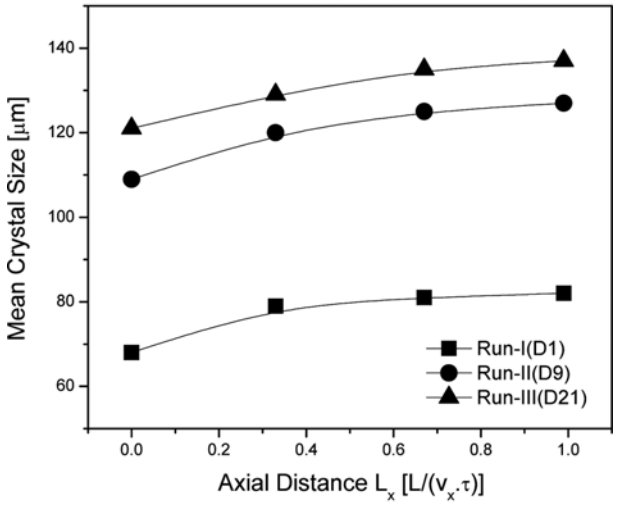

(b)

Fig. 5. Typical axial profile of properties of L-Lysine crystals along axial direction of CT crystallizer when varying multiple feeding mode strategy with 50 °C feed solution temperature, 20 °C cooling temperature, 700 rpm rotation speed for inner cylinder, 900 g/*l* L-Lysine feed concentration, and 5-min mean residence time. (a) Solute concentration and (b) mean crystal size.

the crystal recovery remained almost invariant when varying the multiple feeding mode strategy (Table 1). Yet, the crystal size and crystal size distribution were significantly enhanced when using a suitable multiple feeding mode strategy.

As shown in Fig. 4, the effect of the feeding mode strategy on the crystal size and size distribution in the CT crystallizer was also visually confirmed by microscopic images under the same crystallization conditions as those in Fig. 3. The microscopic observations supported the measurements of the crystal size and crystal size distribution (CV) when using the different feeding mode strategies in the CT crystallizer.

To understand the influence of the multiple feeding mode strategy on the crystal size and crystal size distribution (CV), the crystallization profiles along the axial direction of the CT crystallizer were investigated at the steady state, as shown in Fig. 5. When varying the multiple feeding mode strategy, the solute concentration at the inlet port (L_X=0) of region 1 was much lower than the feed concentration of 900 g/*l*. This result indicates that the L-lysine crystals were quickly crystallized when the feed solution entered the crystallizer, and then became the seed crystals that grew by consuming the solute in the solution, thereby gradually reducing the solute

Table 2. Influence of typical multiple feeding mode strategy on supersaturation in each region (1-3) of CT crystallizer

Experiments	Distributed ratio F1 : F2 : F3	Flow rate of feed solution F1 [ml/min]	Flow rate of feed solution F2 [ml/min]	Flow rate of feed solution F3 [ml/min]	Region 1: $\Delta S1=F(C_{feed}-C_{S1})$ [g/min]	Region 2: $\Delta S2=F(C_{feed}-C_{S2})$ [g/min]	Region 3: $\Delta S3=F(C_{feed}-C_{S3})$ [g/min]
Run-I(D1)	1 : 0 : 0	39.2	0	0	9.996	0	0
Run-II(D3)	0.2 : 0.8 : 0	7.84	31.36	0	2.045	8.211	0
Run-II(D9)	0.8 : 0.2 : 0	31.36	7.84	0	8.073	2.050	0
Run-III(D12)	0 : 1 : 0.2 : 0.7	3.92	7.84	27.44	1.038	2.061	7.099
Run-III(D21)	0.7 : 0.2 : 0.1	27.44	7.84	3.92	7.094	2.062	1.025
Run-III(D22)	0.8 : 0.1 : 0.1	31.36	3.92	3.92	8.039	1.032	1.028

concentration in region 1 (Fig. 5(a)). When using the multiple feeding mode Run-III (D21) and Run-II (D9), since the seed crystals were unable to consume all the solute molecules generated by the distributed feeding along the axial positions, the solute concentration slightly increased in these regions. Meanwhile, when using conventional feeding mode Run-I (D1), the solute concentration was gradually reduced due to the growth of the seed crystals across all the regions in the crystallizer. For all the feeding mode strategies, the mean crystal size became larger along the axial direction of the crystallizer due to crystal growth (Fig. 5(b)). As shown in Table 2, the various feeding mode strategies provided different initial and axial supersaturations. For example, the low initial supersaturation of Run-III (D21) initiated a low nucleation rate, resulting in a small number of seed crystals that continuously grew by consuming the solute in the low supersaturation of the feeding solution (F2 and F3) at regions 2 and 3. Here, the initial and axial supersaturation was an important factor controlling the amount of seed crystals in the first region and the crystal growth and secondary

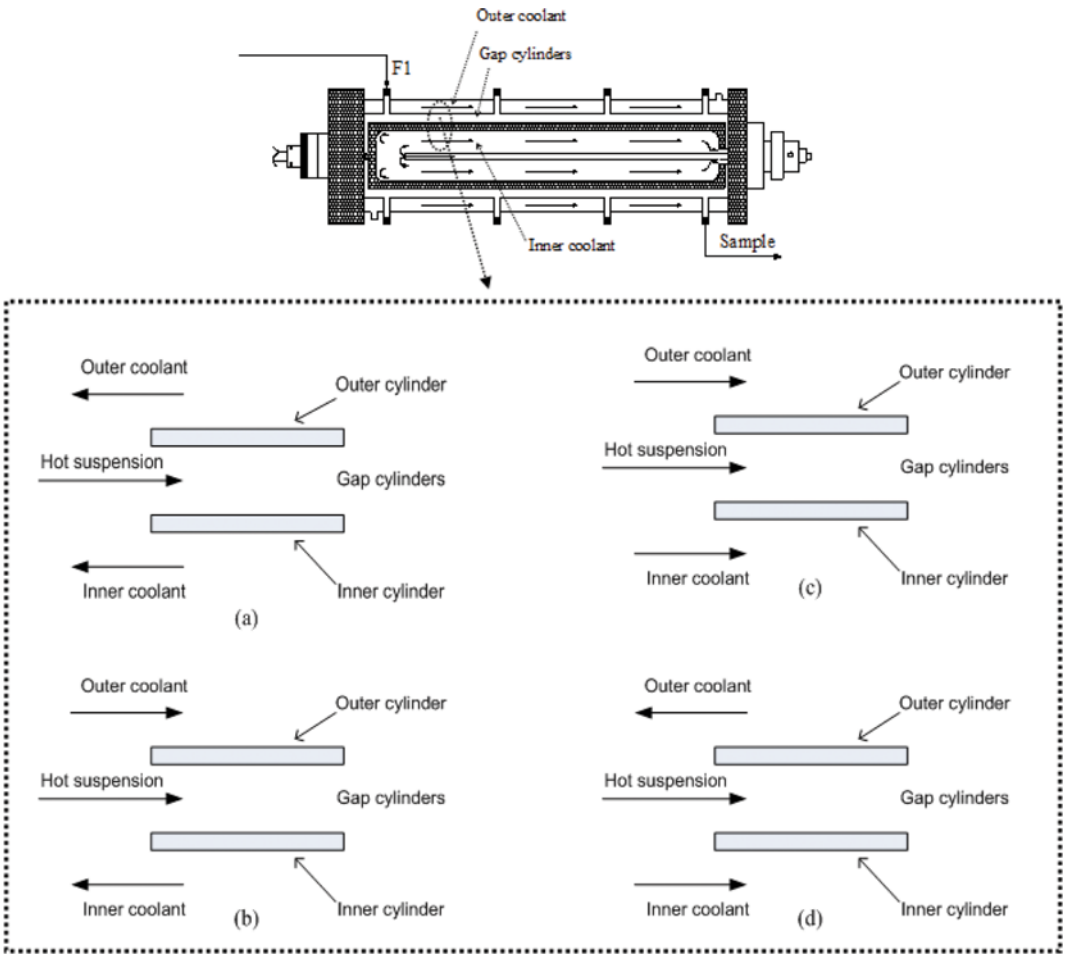

Fig. 6. Schematic of coolant direction strategy of Run-III(D21) in Couette-Taylor crystallizer (a) coolant direction strategy-H_1, (b) coolant direction strategy-H_2, (c) coolant direction strategy-H_3, and (d) coolant direction strategy-H_4.

nucleation in the second and third regions, respectively. Thus, when the supersaturations were initially lower, the mean crystal size and crystal size distribution were enhanced. Consequently, according to the experimental results, feeding mode Run-III (D21) was identified as the optimized feeding strategy for a large mean crystal size with a narrow crystal size distribution in the cooling crystallization of L-lysine.

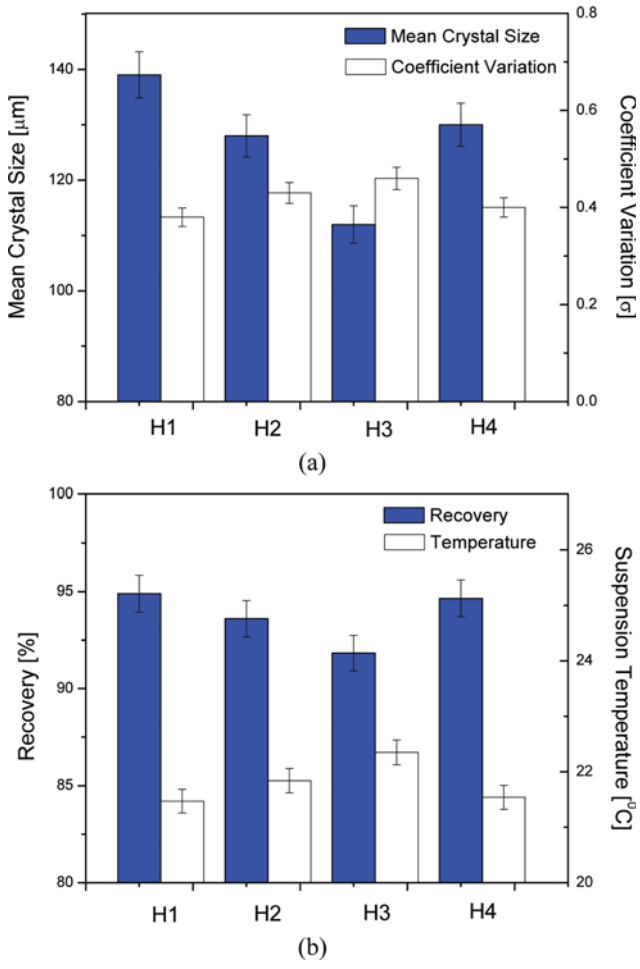

Fig. 7. Influence of coolant direction on crystal size and size distribution of L-Lysine crystals in cooling crystallization of CT crystallizer with 50 °C feed solution temperature, 20 °C cooling temperature, 700 rpm rotation speed for inner cylinder, 900 g/*l* L-Lysine feed concentration, and 5-min mean residence time.

2. Effect of Operating Conditions

Based on the optimized multiple feeding mode strategy for large mean crystal size and narrow crystal size distribution, feeding mode Run-III (D21) was then applied to investigate the influence of the operation conditions, including the coolant direction, rotation speed of the inner cylinder, feed concentration, mean residence time, and cooling temperature on the crystal size, crystal size distribution, and crystal recovery at the steady state. Since the heat transfer between the coolant and the suspension is an important factor controlling the supersaturation during cooling crystallization, the effect of various heat transfers (counter and parallel flows) on the crystals of L-lysine was investigated, as shown in Fig. 6. Here, the flow directions of the inner and outer coolants were adjusted to the opposite and the same flow direction of the feed solution, while the flow rate of the outer and inner coolant remained fixed for all options (H_1-H_4). As shown in Fig. 7, H_1 provided a large mean crystal size with a narrow crystal size distribution (small CV). Meanwhile, the mean crystal size and CV with H_3 were small and large, respectively. This result can be explained in terms of the initial supersaturation in the inlet region (L_X=0) of the CT crystallizer. As shown in Table 3, the initial supersaturation ΔT (L_X=0) clearly depended on the coolant direction with the order $\Delta T_{H3}>\Delta T_{H2}>\Delta T_{H4}>\Delta T_{H1}$, which originated from the different quantities of heat transfer with the order $dQ_1<dQ_4<dQ_2<dQ_3$ (Supporting Information Fig. S1). Thus, the low initial supersaturation with H_1 option provided a low nucleation rate and neglected secondary nucleation, resulting in large mean crystal size with small CV of crystal size distribution. Moreover, the high initial supersaturation with the H_3 option clearly produced small mean crystal size and large CV.

The effect of the cooling temperature on the crystal properties was also investigated, as shown in Fig. 8. Here, when increasing the supersaturation from 25 °C to 35 °C, corresponding to decreasing the cooling temperature, the mean crystal size and CV of the crystal size distribution decreased from 147 μm to 120 μm and 0.39 to 0.36, respectively. Evidently, the nucleation rate was facilitated when increasing the supersaturation, thereby decreasing the mean crystal size. In addition, when increasing the supersaturation, secondary nucleation was promoted, which resulted in larger CV of crystal size distribution (Fig. 8(a)). Moreover, since the solubility of L-lysine crystals depends on the temperature [13], when the cooling temperature decreased, the amount of crystals was enhanced, which explains the increased crystal recovery when increasing the supersaturation, as shown in Fig. 8(b).

Since the nucleation and growth depend obviously on the fluid hydrodynamics and supersaturation of the solution, the influence

Table 3. Influence of coolant direction strategy on quantity of heat transfer and initial supersaturation in inlet region (L_X=0) of Run-III(D21) in CT crystallizer

Coolant direction strategy	Feed temperature T_{feed} [°C]	Outer coolant temperature Toc [°C]	Inner coolant temperature Tic [°C]	Quantity of heat transfer $dQ/(k'\cdot dx)\cdot 10^2$ [°C·m]	Suspension temperature T_S [°C]	Initial supersaturation $\Delta T=T_{feed}-T_S$ [°C]
H1	50	20.75	20.58	152.5	24.92	25.08
H2	50	20.13	20.56	154.3	24.56	25.44
H3	50	20.07	20.0	155.8	24.02	25.98
H4	50	20.73	20.02	153.9	24.76	25.24

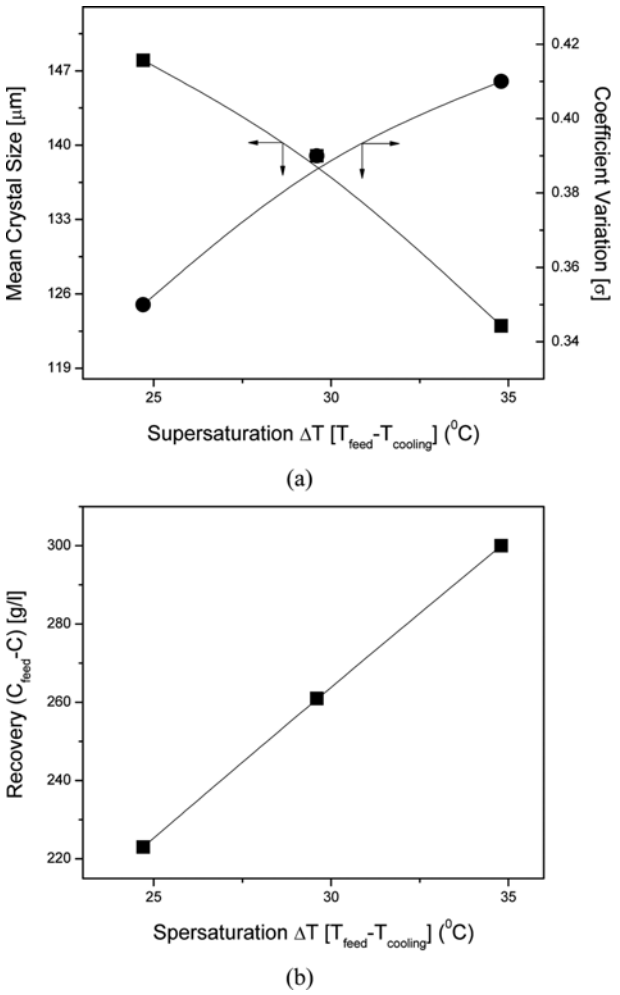

Fig. 8. Influence of cooling temperature on properties of L-Lysine crystals in cooling crystallization of CT crystallizer with 50 °C feed solution temperature, 700 rpm rotation speed for inner cylinder, 900 g/*l* L-Lysine feed concentration, and 5-min mean residence time. (a) Mean crystal size and COV and (b) recovery and suspension temperature.

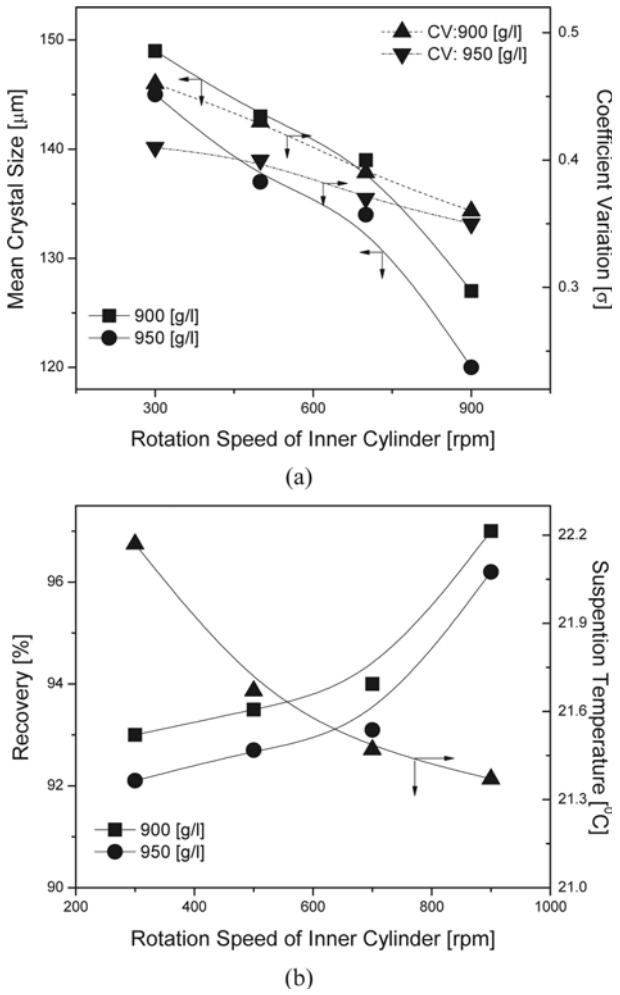

Fig. 9. Influence of rotation speed and feed concentration on properties of L-Lysine crystals in cooling crystallization of CT crystallizer with 50 °C feed solution temperature, 20 °C cooling temperature, 700 rpm rotation speed for inner cylinder, 900 g/*l* L-Lysine feed concentration, and 5-min mean residence time. (a) Mean crystal size and COV and (b) recovery and suspension temperature.

of the rotation speed of the inner cylinder and feed concentration on the mean crystal size and CV of crystal size distribution of the L-lysine was also investigated. As shown in Fig. 9(a), the mean crystal size and CV decreased from 149 μm to 127 μm and 0.46 to 0.36, respectively, when increasing the rotation speed of the inner cylinder from 300 rpm to 900 rpm. Here, the heat and mass transfer in the Taylor vortex flow was enhanced when increasing the rotation speed, which promoted the supersaturation and nucleation rate, resulting in a decreased crystal size [13]. In addition, the high nucleation rate provided the large surface area of crystals, which rapidly decreased the supersaturation, resulting in small CV of crystal size distribution. As shown in Fig. 9(b), the crystal recovery was also enhanced from 93% to 97% when increasing the rotation speed. This was due to the promotion of the nucleation and growth when increasing the rotation speed, resulting in an enhanced crystal recovery. This dependency of the mean crystal size and crystal size distribution on the supersaturation was also confirmed when varying the feed concentration, as shown in Fig. 9(a). Essentially, increasing feed concentration provided a higher supersaturation causing an enhanced nucleation, resulting in decrease of mean crystal size and CV of crystal size distribution. Moreover, the crystal recovery was reduced when increasing the feed concentration, as shown in Fig. 9(b). This indicates that the crystal recovery was critically determined by the crystal growth, which was controlled by the mass transfer in the Taylor vortex flow. That is, when varying the feed concentration at a fixed rotation speed of the inner cylinder, the consumption of solute molecules by the crystal growth was not so much changed. So, the crystal recovery was reduced as increasing the feed concentration.

As shown in Fig. 10, the effect of the mean residence time on the mean crystal size, crystal size distribution (CV), and crystal recovery was also investigated. It is already known that the feed flow rate directly influences the supersaturation in continuous operation of crystallization. When increasing the mean residence time from 1 min to 15 min (decreasing of feed flow rate), the mean crys-

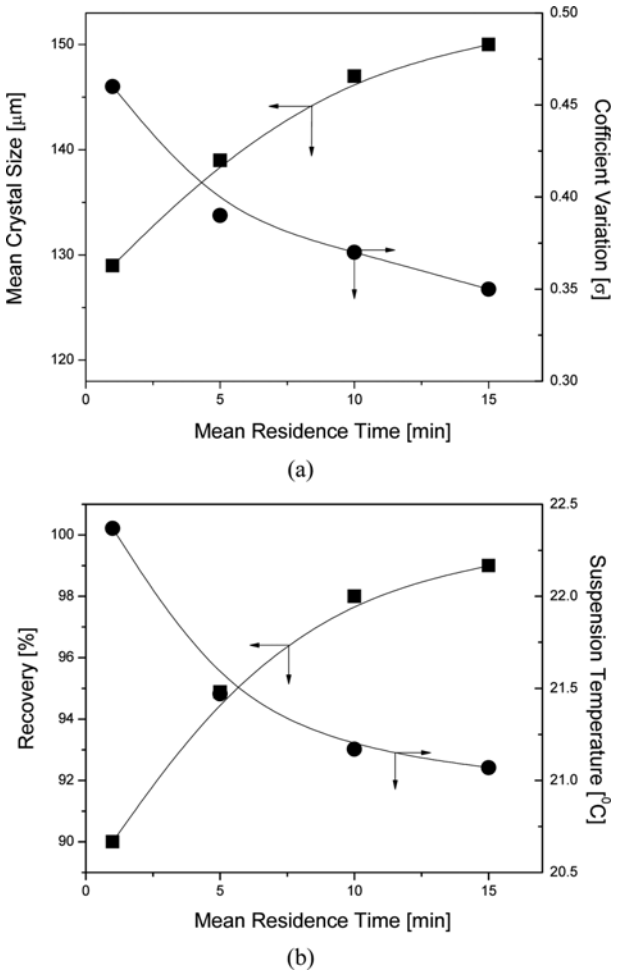

Fig. 10. Influence of mean residence time on the properties of L-Lysine crystals in cooling crystallization of CT crystallizer with 50 °C for feed solution temperature, 20 °C for cooling temperature, 700 rpm rotation speed for inner cylinder, 900 g/*l* L-Lysine feed concentration and 5 min mean residence time. (a) mean crystal size and COV and (b) recovery and suspension temperature.

tal size increased from 129 μm to 150 μm, while the crystal recovery was enhanced from 90% to 99%. In addition, the CV of the crystal size distribution decreased from 0.46 to 0.35. The explanation is that the long mean residence time (low feed flow rate) provided the low supersaturation and caused the low nucleation rate, resulting in large mean crystal size. Also, the secondary nucleation was suppressed during the crystallization, contributing to the small CV of crystal size distribution (Fig. 10(a)). In addition, with decreasing the feed flow rate (increasing the mean residence time), it provided higher heat and mass transfers in continuous Taylor vortex flow [14,15]. Thus, the crystal recovery was enhanced and the suspension temperature was lowered, as shown in Fig. 10(b).

CONCLUSION

The present study demonstrates the effect of a multiple feeding mode strategy on the mean crystal size and crystal size distribution of L-lysine in the CT crystallizer. When compared with the conventional feeding mode (Run-I (D1)), the multiple feeding mode strategy (Run-II or Run-III) was shown to be a useful technique for enhancing the mean crystal size and crystal size distribution by controlling the supersaturation in each region of the crystallizer. Here, the optimized multiple feeding mode strategy was defined as Run-III (D21) with a feeding ratio of $F_1 : F_2 : F_3 = 0.7 : 0.2 : 0.1$, which produced the largest mean crystal size with the narrowest crystal size distribution.

ACKNOWLEDGEMENTS

This work was supported by the Engineering Research Center of the Excellence Program of the Korean Ministry of Science, ICT & Future Planning (MSIP)/National Research Foundation of Korea (NRF) (Grant NRF-2014R1A5A1009799).

SUPPORTING INFORMATION

Additional information as noted in the text. This information is available via the Internet at http://www.springer.com/chemistry/journal/11814.

REFERENCES

1. A. S. Myerson, *Handbook of Industrial Crystallization*, Butterworth-Heinemann, Oxford (1993).
2. K. Shimiza, T. Nomura and K. Takahashi, *J. Cryst. Growth*, **191**, 178 (1998).
3. V. Liotta and V. Sabesan, *Org. Proc. Res. Dev.*, **8**, 488 (2004).
4. N. Kubota, N. Doki, M. Yokota and D. Jagadesh, *J. Chem. Eng. Japan*, **35**, 1063 (2002).
5. R. Davey and J. Garside, *From Molecules to Crystallizers*, Oxford University Press, New York (2000).
6. G. Shan, K. Igarashi, H. Noda and H. Ooshima, *Chem. Eng. J.*, **85**, 161 (2002).
7. H. Takiyama, K. Shindo and M. Matsuoka, *J. Chem. Eng. Japan*, **35**, 1072 (2002).
8. D. Y. Kim and D. R. Yang, *Korean J. Chem. Eng.*, **32**, 1222 (2015).
9. A.-T. Nguyen, J. M. Kim, S. M. Chang and W.-S. Kim, *Ind. Eng. Chem. Res.*, **49**, 4865 (2010).
10. S. Lee, A. Choi, W.-S. Kim and A. S. Myerson, *Cryt. Growth Des.*, **11**, 5019 (2011).
11. J. M. Kim, S. M. Chang, J. H. Chang and W.-S. Kim, *Colloids Surface A: Phys. Eng. Asp.*, **384**, 31 (2011).
12. S. Lee, C. H. Lee and W.-S. Kim, *J. Cryst. Growth*, **373**, 32 (2012).
13. A.-T. Nguyen, T. Yu and W.-S. Kim, *J. Crys. Growth*, DOI:10.1016/j.jcrysgro.2016.10.020 (2017).
14. A.-T. Nguyen, Y. L. Joo, S. M. Chang and W.-S. Kim, *Cryt. Growth Des.*, **12**, 2780 (2012).
15. W. L. McCabe, J. C. Smith and P. Harriott, *Unit Operations of Chemical Engineering 6th*, McGraw Hill, Boston (2001).

Supporting Information

Influence of feeding mode on cooling crystallization of L-lysine in Couette-Taylor crystallizer

Anh-Tuan Nguyen and Woo-Sik Kim†

Department of Chemical Engineering, ILRI, Kyung Hee University, Seocheon-dong, Giheung-gu, Yongin-si 17104, Korea
(*Received 25 Novembr 2016 • accepted 16 March 2017*)

The quantity of heat transferred in the unit time through surface area dA (m^2) is defined as,

$$dQ=kdA(T_{h(t)}-T_{coolant}) \quad (s.1)$$

This heat is extracted from the suspension by the coolant. Here, $T_{h(t)}$ and $T_{coolant}$ are the suspension and coolant temperature, respectively. In addition, k ($W/m^2 \cdot K$) is the overall heat transfer coefficient that is assumed a constant and defined as [14]

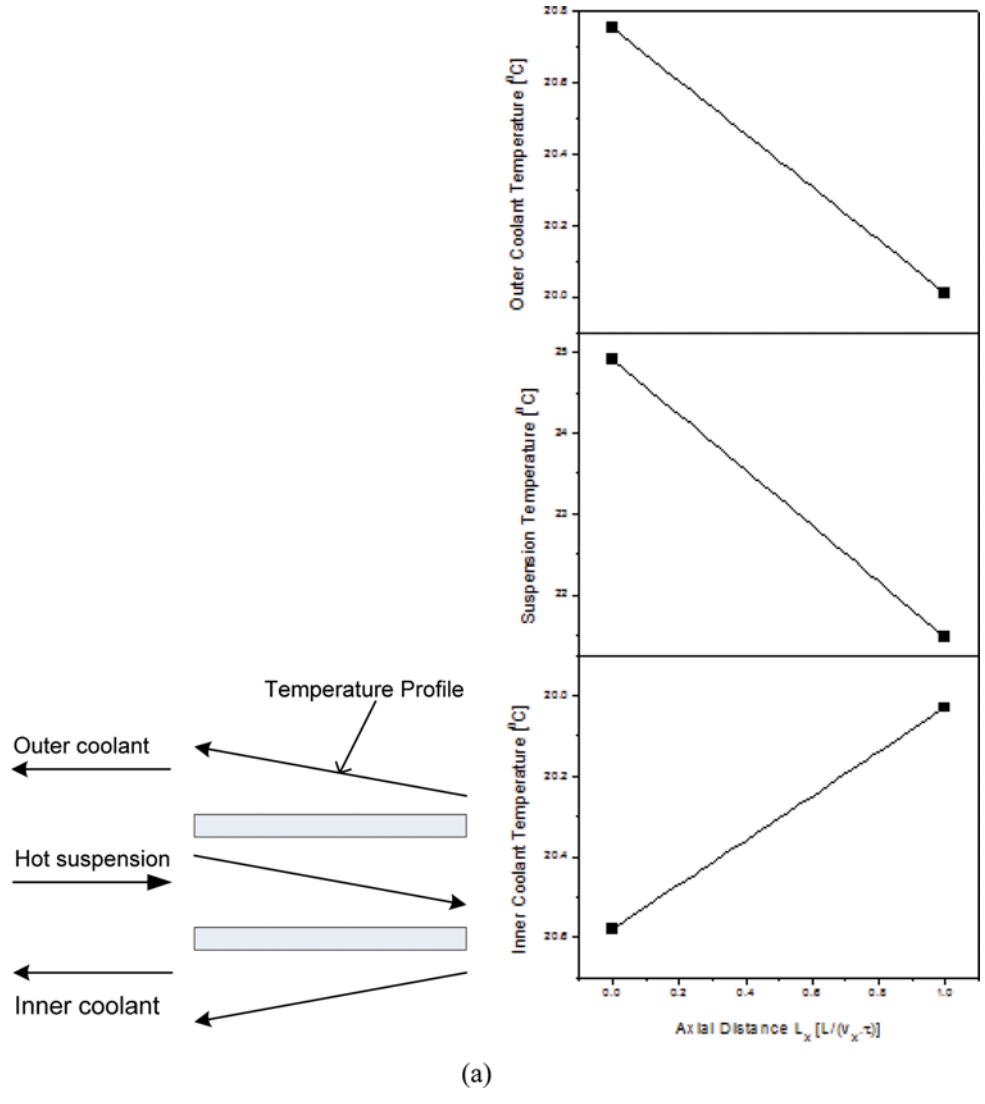

Fig. S1. Influence of coolant direction on suspension temperature of L-Lysine products in Run-III(D21) of CT crystallizer with 50 °C feed solution temperature, 700 rpm rotation speed for inner cylinder, 900 g/*l* L-Lysine feed concentration, and 5-min mean residence time. (a) Coolant direction-H_1, (b) coolant direction-H_2, (c) coolant direction-H_3, and (d) coolant direction-H_4.

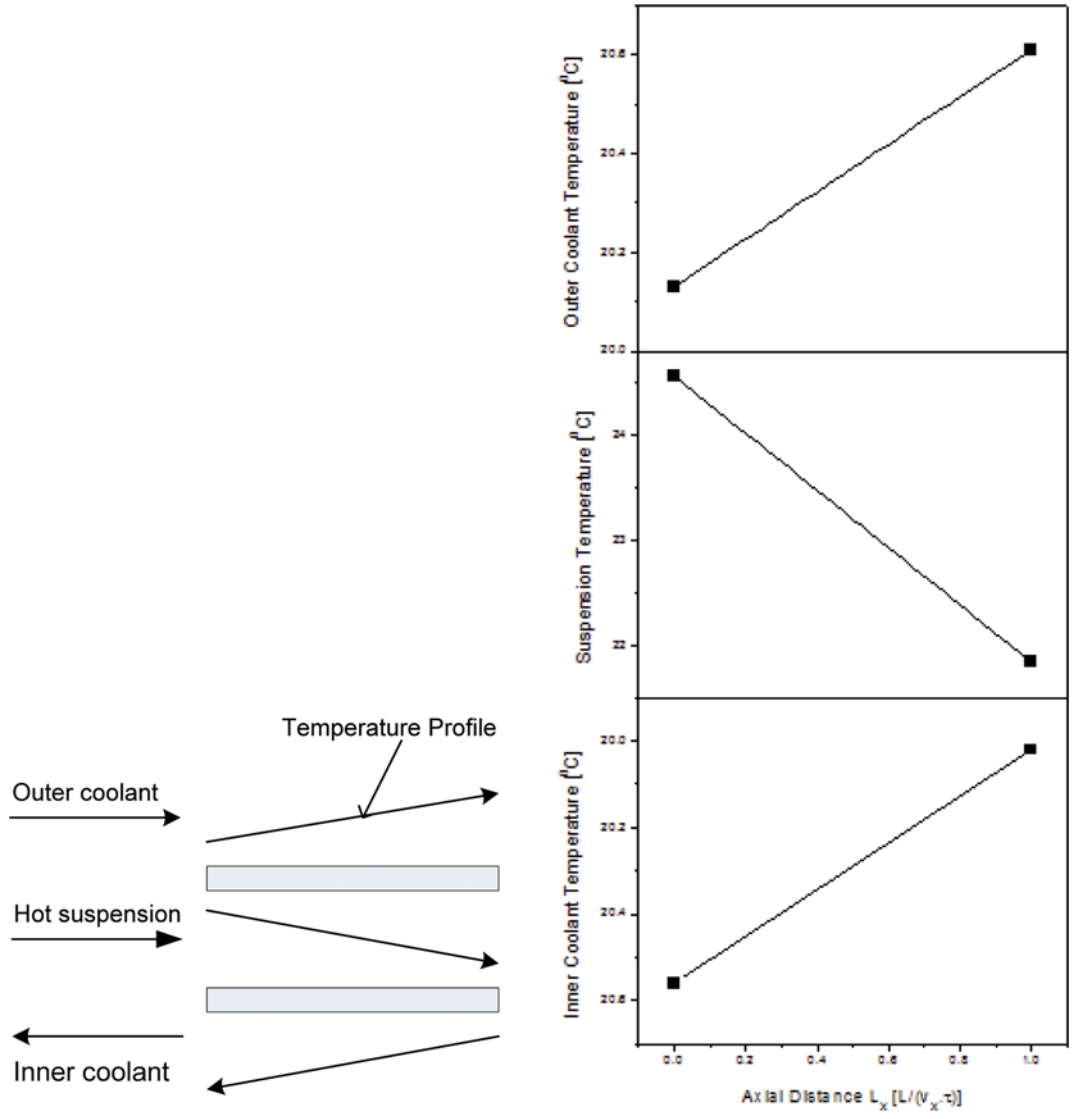

(b)

Fig. S1. Continued.

$$k = \frac{1}{\frac{1}{h_i} + a\frac{x_w}{k_m} + \frac{1}{h_o}} \quad \text{(s.2)}$$

where, h_i and h_o are the individual heat-transfer film coefficients inside and outside the wall, respectively, which are defined as $h_i=(dQ/dA)/(T_h-T_w)$ and $h_o=(dQ/dA)/(T_w-T_c)$, respectively. Also, x_w and k_m are the thickness and thermal conductivity of the wall, respectively.

For the outer cylinder heat transfer, the quantity of heat transferred is defined as

$$dQ_o=kdA_o(T_{h(t)}-T_{Outercoolant})=k'r_o dx(T_{h(t)}-T_{Outercoolant}) \quad \text{(s.3)}$$

For the inner cylinder heat transfer, the quantity of heat transferred is defined as

$$dQ_i=kdA_i(T_{h(t)}-T_{Innercoolant})=k'r_i dx(T_{h(t)}-T_{Innercoolant}) \quad \text{(s.4)}$$

where, r_o and r_i are the radius of the outer and inner cylinder of the CT crystallizer, respectively. Thus, the total quantity of heat transferred is

$$dQ=dQ_o+dQ_i=k'dx[T_{h(t)}(r_o+r_i)-(r_oT_{Outercoolant}+r_iT_{Innercoolant})] \quad \text{(s.5)}$$

From Eq. (s.5), when the temperature of feed solution was fixed at $T_{feed}=T_{h(t=0)}=50\,^{\circ}C$, the quantity of heat transfer at the inlet point ($L_X=0$) clearly depended on the outer and inner coolant temperatures ($T_{Outercoolant(L=0)}$, $T_{Innercoolant(L=0)}$). Thus, the initial supersaturation ΔT ($T_{feed}-T_{h(t)}$) in the inlet region depended on the direction of the coolant, as shown in Fig. S1.

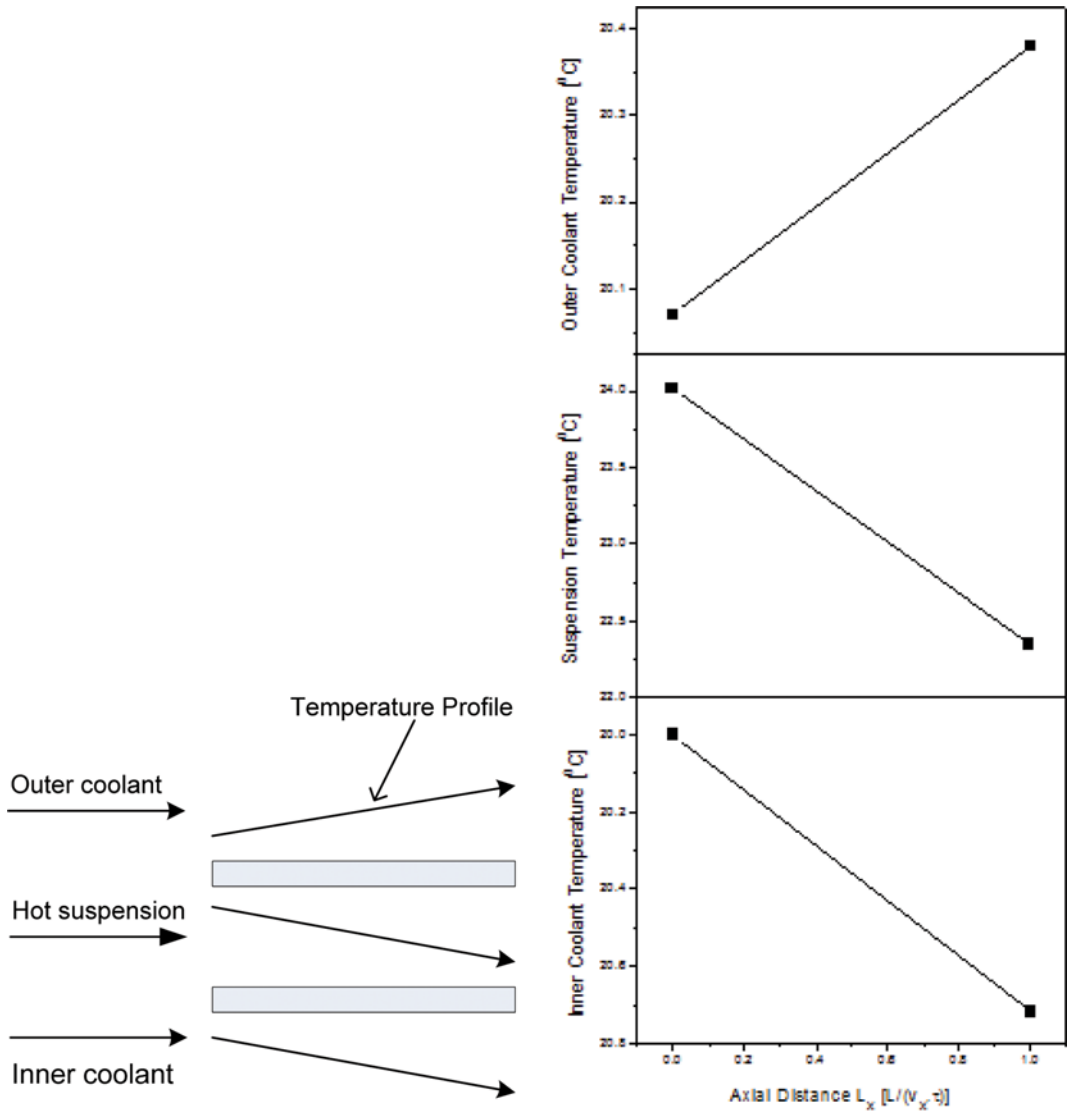

(c)

Fig. S1. Continued.

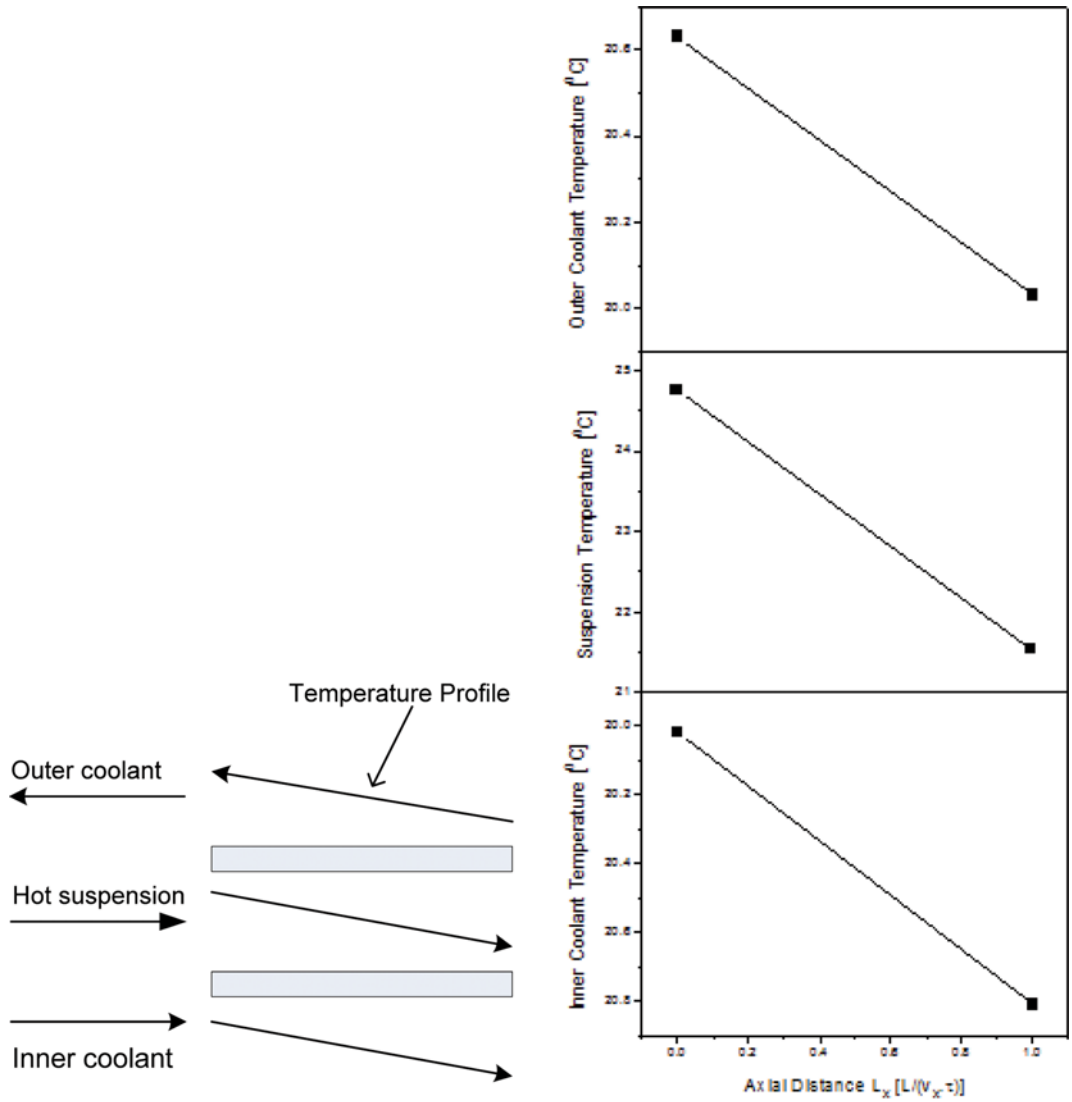

(d)

Fig. S1. Continued.